View metadata, citation and similar papers at core.ac.uk
brought to you by CORE
provided by RERO DOC Digital Library

Anal Bioanal Chem (2004) 378 : 1069–1074
DOI 10.1007/s00216-003-2346-7

SPECIAL ISSUE PAPER

Hans-Rudolf Kuhn · Marcel Guillong · Detlef Günther

Size-related vaporisation and ionisation of laser-induced glass particles in the inductively coupled plasma

Received: 3 June 2003 / Revised: 22 September 2003 / Accepted: 14 October 2003 / Published online: 5 December 2003
© Springer-Verlag 2003

Abstract Ongoing discussions about the origin of elemental fractionation occurring during LA-ICP-MS analysis show that this problem is still far from being well understood. It is becoming accepted that all three possible sources (ablation, transport, excitation) contribute to elemental fractionation. However, experimental data about the vaporisation size limit of different particles in the ICP, as produced in laser ablation, have not been available until now. This information should allow one to determine the signal contributing mass within the ICP and would further clarify demands on suitable laser ablation systems and gas atmospheres in terms of their particle size distribution.

The results presented here show a vaporisation size limit of laser induced particles, which was found at particle sizes between 90 nm and 150 nm using an Elan 6000 ICP-MS. Due to the fact that the ICP-MS response was used as evaluation parameter, vaporisation and ionisation limits are not distinguishable.

The upper limit was determined by successively removing the larger particles from the aerosol, which was created by ablation of a NIST 610 glass standard at a wavelength of 266 nm, using a recently developed particle separation device. Various particle fractions were separated from the aerosol entering the ICP. The decrease in signal intensity is not proportional to the decrease in volume, indicating that particles above 150 nm in diameter are not completely ionised in the ICP. Due to the limited removal range of the particle separation device, which cannot remove particles smaller than 150 nm, single hole ablations were used to determine the lower vaporisation limit. This is based on measurements showing that larger particles occur dominantly during the first 100 laser pulses only. After this period, the ratio of ICP-MS counts and total particle volume was found to be constant while most of the particles are smaller than 90 nm, indicating complete vaporisation and ionisation of these particles.

To describe the influence of different plasma forward powers on the vaporisation limit, the range 1000–1600 W was studied. Results indicate that optimum vaporisation and ionisation occurs at 1300 W. However, an increase of the particle ionisation limit towards larger particles was not observed within the accuracy of this study using the full range of parameters available for optimisation on commonly used ICP-MS instruments.

Keywords Laser-ablation-ICP-MS · Ionisation · Plasma · Particles · Aerosol

H.-R. Kuhn · M. Guillong · D. Günther (✉)
Laboratory for Inorganic Chemistry,
Swiss Federal Institute of Technology (ETH Zürich),
HCI G113, Hönggerberg, 8093 Zürich, Switzerland
e-mail: guenther@inorg.chem.ethz.ch

Introduction

Laser ablation inductively coupled plasma mass spectrometry (LA-ICP-MS) is an established technique for the analysis of a wide variety of samples in geology, chemistry, metallurgy and biology (ref. [1] and references therein). Beside of major advantages like spatial resolution and low sample preparation, the limits of detection and signal stabilities are still not as good as those achievable by using solution nebulization ICP-MS in terms of mass loss in the ablation cell, transport tube and during the excitation.

A lot of effort has been made to improve sensitivity in LA-ICP-MS. Most of the work carried out focused on the sampling in terms of the laser wavelengths [2, 3], pulse duration [4], carrier gas [5] and ablation cell design [6] as significant parameters to influence aerosol properties. The ICP itself is routinely used as an efficient excitation source and almost no significant changes to the ICP have been made for direct solid sampling. However, the introduction of a laser-generated aerosol into two different ICP instruments led to significant different signal response, which indicated that the ionisation efficiency is not the same for all ICP sources [7]. Furthermore, optimum ion sampling occurs at different positions inside the ICP and is therefore not the same for different elements, especially for aerosols containing larger particles [8, 9].

Different authors predicted the ICP as one source also responsible for elemental fractionation [10, 11], especially if particles larger than 1 µm (glass samples [12]) and 400 nm (metals [13]) are introduced. ICP-MS response curves of solution nebulization aerosols differ substantially from laser aerosols, indicating different excitation behaviour of droplets and particles in the ICP [14]. Russo et al. [15] reported anomalous elemental ratios measured after the first laser pulse, where significantly larger particles are produced compared to the following laser pulses, which can be interpreted as incomplete ionisation in the ICP. Therefore, we conclude that amongst other sources, elemental fractionation also occurs in the ICP-MS due to incomplete vaporisation, atomisation and ionisation of these particles, whereby the more volatile species could be enriched in smaller particle size fractions and on particle surfaces during particle formation, which leads to different vaporisation efficiencies in the ICP. However, even stoichiometric sampling into a broad range of particle sizes could enhance similar effects.

The critical particle size completely vaporised and ionised in the ICP has not been determined for solids so far. In 1994, Olesik et al. [16] introduced well-defined aqueous droplets into the inductively coupled plasma and found their ionisation limit at 10–15 µm. Knight et al. [17] described incomplete ionisation of spherical glass particles within a size range of 3–7 µm, and Guillong et al. [12] described incomplete ionisation of an aerosol produced by a 266-nm laser from a glass sample. By determining ablation rates of NIST 610, 612 and 614 glass standards using standardised 266-nm laser ablation parameters, two times lower sensitivities for two times more ablated mass have been found for the more transparent samples (e.g. NIST 612, 614) [18]. This discrepancy can be explained by highly variable particle sizes measured in aerosols for all three samples [19], where more opaque samples with a lower penetration depth produce smaller particles than transparent samples. Furthermore, the particle size distribution depends strongly on the ablation environment [5]. The formation of particles is not completely known. However, the bimodal particle size function measured on Cu [20] indicates that three types of particles might occur (vapour condensation particles, clusters and cracked or splashed particles). Furthermore, studies on brass [13] showed laser-induced fractionation into different particle size fractions, which is superimposed by incomplete ionisation of particles larger than 400 nm entering the ICP. Recently, Aeschliman and co-worker [21] recorded high-speed camera pictures of laser aerosols introduced into an ICP. The aerosol structure and the lifetime of particles within the ICP indicate that only a small portion of the particles vaporises completely.

The present study was carried out to determine the vaporisation and ionisation size limit of glass particles under various plasma conditions to gain further insights into solid particle vaporisation and ionisation behaviour in the ICP. Furthermore, different plasma forward power settings were applied to investigate the influence of ICP optimisation on the ionisation efficiency.

Experimental

Instrumentation

The laser-induced aerosol was generated using an LSX 200+ laser ablation system (Cetac Technologies, Omaha, NB), which is based on a Nd:YAG solid-state laser operating at 266 nm (4th harmonics). This laser ablation system provides an aerosol with a wide particle size distribution as required for such experiments. An in-house-built, leak-proof ablation cell with a volume of approximately 30 cm^3 was used to ensure a constant gas flow independent from the slightly raised carrier gas backpressure caused by the particle separation device.

The recently described particle separation device [22] was located 50 cm after the ablation cell. For particle separation, a 1-m-long silicon tubing (i.d. 1 mm), which was wrapped several times around a glass rod, (diameter 8 mm) was used. This arrangement allows one to adjust the particle size cut off over a wide range. The effective cut off was defined as the size where the measured number of particles was reduced by one order of magnitude. For reasons reported elsewhere [22], helium was always used as aerosol carrier at a flow rate of 1.7 L min^{-1}. The unusually high flow rate was applied to achieve optimum separation of particles within the separation device. In all experiments without particle separation, the same set-up was used with a straight silicon tube, where only few of the largest particles from the aerosol were lost.

The aerosol from the separation device was split into two parts using a Y-piece. A flow of 0.2 L min^{-1} was directed to a particle measurement system and the remaining 1.5 L min^{-1} to the ICP-MS (Elan 6000, Perkin–Elmer, Norwalk, CT). Particle size measurements were carried out using an HS-LAS (Particle Measuring Systems, Denver, CO, USA), which is a 32-channel instrument based on laser light scattering. The instrument covers a size range between 65 nm and 1 µm. The aerosol flow rate through the instrument was adjusted internally to 0.2 L min^{-1}. The instrument was calibrated using latex spheres as a standard. Spherical glass particles produced in laser ablation have slightly different light scattering properties. Therefore, the absolute size measurements deviate in a range of approximately less than 10%. This instrumental uncertainty is the same for all measurements and is therefore not considered in the standard deviations shown in the figures.

Sample and experimental conditions

All experiments were carried out three times using a polished NIST 610 glass standard. This standard contains relatively high amounts of trace elements, resulting in a reasonable ICP-MS signal under the experimental conditions used. To avoid overloading effects of the particle measurement instrument, a laser repetition rate of 1 Hz at a crater size of 50 µm and 100% laser output (energy density of 6 J cm^{-2}) was used. The sample was pre-ablated with 3 pulses before carrying out single hole drilling experiments. Experiments with the particle separation device were carried out using 30 single spot ablation pulses without pre-ablation.

The ICP-MS was operated at three different plasma forward powers to monitor differences in ionisation efficiency. The ablation cell gas helium was admixed with argon before entering the ICP. Optimised argon gas flows have been found to be almost the same for all power settings. The additional gas, which was admixed to the helium gas flow, was changed slightly (1,600 W: 0.9 L min^{-1}, others: 0.85 L min^{-1}) to reach optimum excitation conditions. Auxiliary (0.9 L min^{-1}) and cooling gas flow (16 L min^{-1}) were kept constant. Helium flow rates, which also influence the ICP conditions, had to be kept constant because of the particle separation. An additional vacuum pump was connected to the interface to maintain the vacuum conditions for the helium/argon mixture comparable to argon only.

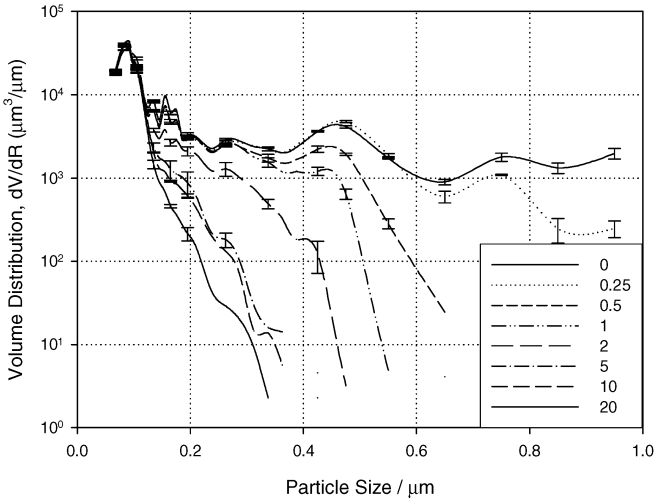

Fig. 1 Particle volume distribution after the particle separation device. The *legend* refers to the numbers of turnings. *Error bars* are given as 1 σ

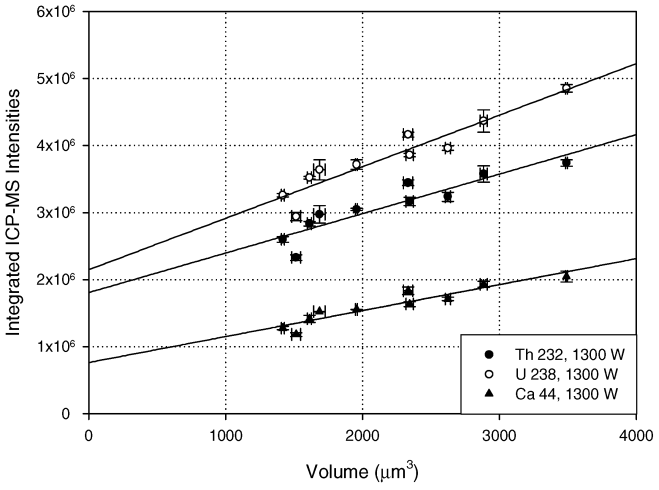

Fig. 2 Integrated ICP-MS signal intensities versus volume for different selected isotopes. Axis intercepts of the linear regressions are non-zero, which would be expected in case of complete vaporisation and ionisation. *Error bars* are given as 1 σ

Results and discussion

The first two sections below show the results using 1300-W plasma power, which is a common value for dry plasma conditions. In the third section, three different plasma forward powers are compared to investigate the influence of plasma conditions on the ionisation efficiency of individual particle size fractions.

Experiments with the particle separation device

The particle separation device allows one to remove a well-defined fraction of larger particles from the aerosol [22] without changing the volume distribution of the smaller particles. The particle size cut off was adjusted by different numbers of turns of the silicon tube. A range from 0.25 to 30 turns was applied, which leads to particle size cut offs from 950 nm down to 150 nm. The particle volume distributions after applying the particle separation device are shown in Fig. 1.

Assuming complete ionisation of all particles, the total particle volume measured should be proportional to the integrated ICP-MS intensities. Experimentally, stepwise lowering of the particle cut off size down to 150 nm reduced the total volume of particles entering the ICP and the particle measurement system. The decrease of the volume was determined to be 60% accompanied by a decrease in integrated ICP-MS signal intensities by 30–40% only (Fig. 2). Axis intercepts of the linear regression curves of intensity and volume for U, Th and Ca are far from zero, indicating incomplete vaporisation and ionisation of the aerosol particles after removing the particle size fraction above 150 nm.

Figure 3 shows the ratios of the integrated ICP-MS signal intensities normalised to the total volume as a function of the cut off size. In the case of complete ionisation the integrated signal intensities per volume would be constant.

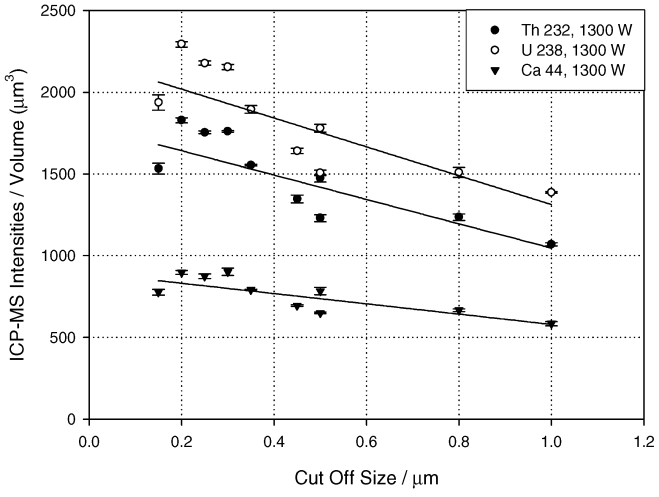

Fig. 3 The ratio of integrated ICP-MS signal intensities and total volume transported is not constant, indicating that the larger particles do not fully contribute to the ICP-MS signal intensities. *Error bars* are given as 1 σ

However, the ratio decreases with larger cut off sizes and indicates that the ICP-MS is not capable of ionising particles above 150 nm completely. For the matrix studied, the particle size limit for complete ionisation is equal to or smaller than 150 nm. Considering the wavelength- and matrix-dependent particle size distribution in laser ablation, it must be concluded that most of the commonly used laser ablation systems produce particle size fractions, which are not fully contributing to signal intensities detected within the ICP-MS.

Single hole drilling

Single hole drilling experiments show that the particle size distribution of the aerosol changes dramatically with in-

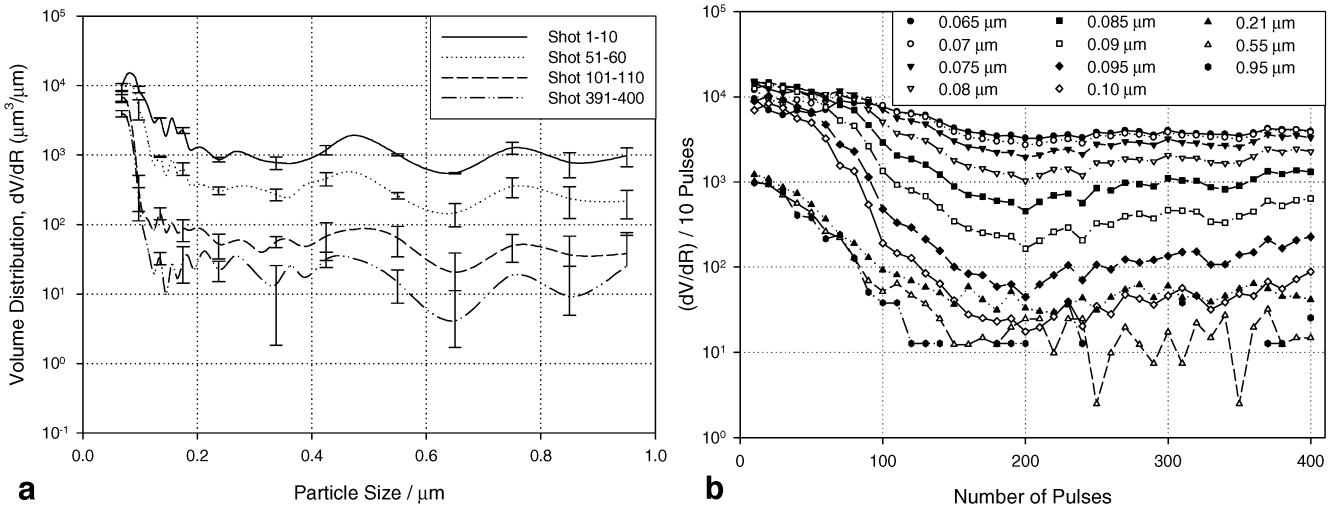

Fig. 4 **a** Selected volume distributions after 10, 60, 110 and 400 laser pulses. *Error bars* (1 σ) are larger for low volumes, because only few particles have been detected. **b** Decrease of particle volumes shown for selected channel sizes of the particle measurement system; numbers of particles larger than 90 nm are reduced far more than particles smaller than 90 nm. In the 0.95 µm channel, single particle counts result in a step-like graph

creasing penetration of the sample. Time-dependent measurements of the particle size distribution show that in the beginning of the ablation a large portion of particles up to 1 µm and possibly larger (limited by the measurement range) are generated by the laser and transported to the ICP-MS. After reaching a crater depth to diameter ratio of approximately 1 this is no longer the case for a NIST 610 sample and the size distribution is shifted towards particles smaller than 90 nm. To achieve the necessary time resolution, the ablation was stopped after every 10 laser pulses and the total numbers of particles together with the ICP-MS signal intensities were recorded simultaneously. Splitting an ablation of 400 laser pulses into 40 single ablations with 10 pulses each neither influences the total transported particle volume nor the total ion counts, which was tested by comparing the integrated signals of the 40 segments with continuous ablation over the same number of laser pulses. Transport efficiency for continuous and segmented ablation was found to be constant and was determined to be overall 9.7±1.0%, which is in good agreement with previously reported values [13, 23].

By ablating the NIST 610 glass using a 50-µm crater, particle volume distribution in the aerosol shows a rapid decrease in the size range between 1 µm and 100 nm. The reduction is variable between the individual channels but includes all measured particle sizes of the given range and exceeds by far an order of magnitude within the first 100 laser pulses. After 100 pulses, few particles larger than 100 nm were detected. Particles below decrease during the entire ablation, but their reduction is significantly lower (see Fig. 4a,b). This experimentally determined time-dependent particle size distribution allowed us to define the particle cut off size at 90 nm. After 100 pulses, the aerosol consists mainly of particles smaller than 90 nm, as shown in Fig. 4b.

Fig. 5 Integrated ICP-MS signal intensities of sodium (**a**) and thorium (**b**) versus total volume transported during a single hole drilling experiment

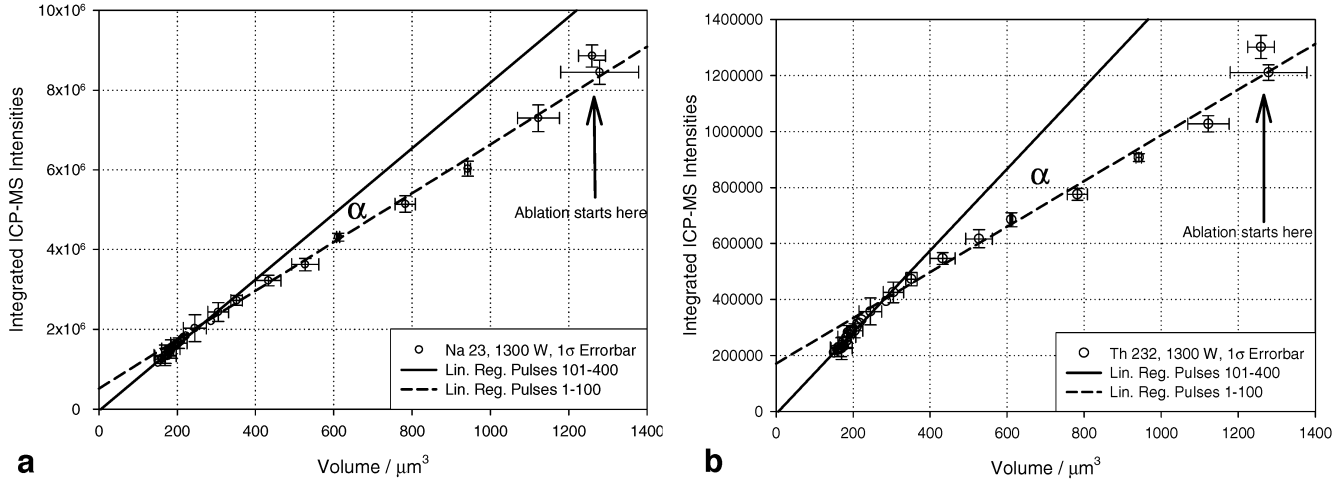

The graph of the integrated ICP-MS signal intensities versus volume shows a significant non-linearity, which occurs between 100 and 120 pulses. It was measured for main elements like sodium and for trace elements like thorium (Fig. 5a,b). Linear regressions of the data points from the first 100 pulses, where large particles are dominant, give an intercept deviating from zero. In contrast, the linear regression through the last 30 data points shows strong correlation and intercepts through zero, indicating that all particle fractions are completely ionised within the ICP. In conclusion, based on the cut off size of 90 nm determined for single hole drilling experiments, particles smaller than approximately 90 nm are completely ionised in the ICP.

The angle between the linear regression slopes of the data points of the first 100 pulses (small and large particle fractions) and pulses 110 to 400 (small particle fractions) was defined to be the vaporisation index (α). This index is element-dependent. In the case of complete vaporisation and ionisation, signal intensities would correlate with the particle volume introduced into the ICP, resulting in a vaporisation index of zero (α=0). This was only observable for Pb, while all other elements show significant deviations from α=0, as shown in Fig. 7.

Furthermore, the vaporisation index pattern in Fig. 7 is an inverse function of the fractionation index calculated relative to Ca published elsewhere [12, 24]. Elements with high fractionation indices similar to Si (e.g. Na, Cu, Sn, Pb and U) show a smaller vaporisation index (α) than elements fractionating like Ca (e.g. Al, Zr, Hf, Ta and Th). This variable particle vaporisation and ionisation efficiency is an indication that elemental fractionation depends amongst other sources (chemical separation into different particle size fractions) strongly on the particle size distribution. Considering this relationship, it becomes clear that the fractionation index calculation relative to Ca leads to accurate values for elements with the same vaporisation index as Ca. In summary, Fig. 7 shows that the offset of the vaporisation index from zero shows incomplete vaporisation and ionisation of particles in the ICP, while the element-dependent pattern represents the sum of laser-induced and ICP-induced elemental fractionation.

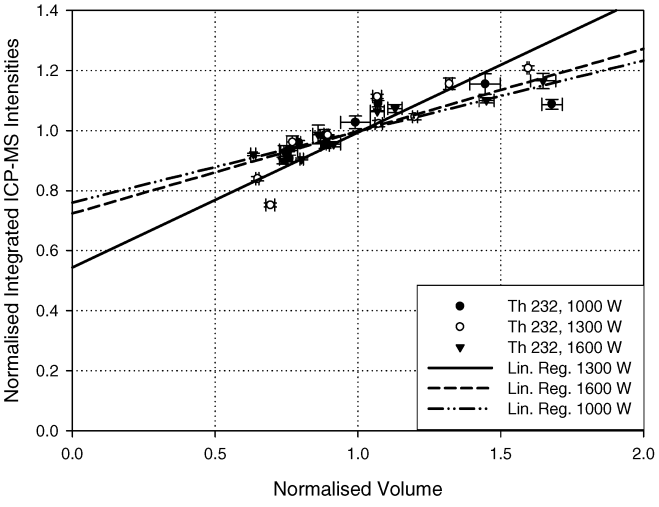

Fig. 6 Integrated ICP-MS signal intensities versus volume using the particle separation device at different plasma power settings. A slightly higher slope and therefore somewhat better ionisation was observed at 1300 W plasma power. Both *axes* are normalised in terms of the mean of all values, 1 σ *error bars*

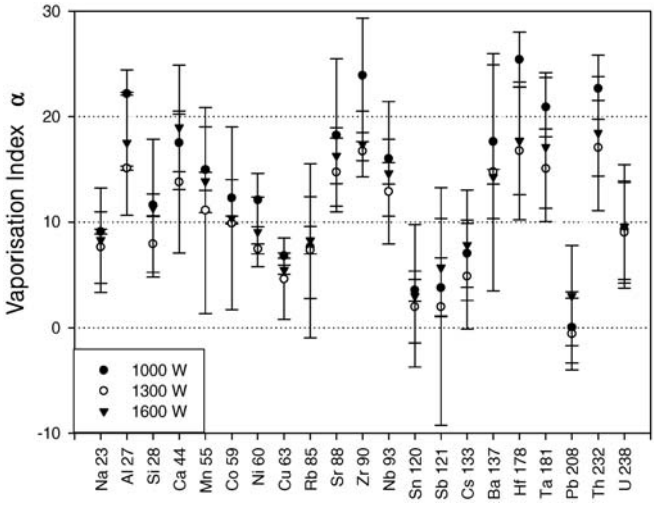

Fig. 7 Vaporisation indices α show significant incomplete ionisation of particles larger than 90 nm (2 σ *error bars*). The highest α was found for 1000 W plasma forward power, indicating better ionisation at higher power settings

Comparison of ionisation efficiencies using different plasma forward powers

The plasma forward power is known to influence the sensitivity in LA-ICP-MS and also affects the ionisation efficiency of different particle sizes. Therefore, three plasma forward powers (1000 W, 1300 W and 1600 W) covering the range of commonly used ICP-MS instrumentation were studied.

Because the present work can only isolate the particle vaporisation and ionisation size limit between an under and an upper particle size, a slight change in the ionisation particle size limit within the given range of 90 nm to 150 nm cannot be resolved. Experimental data using the particle separation device show a dependence of the particle ionisation efficiency on the plasma forward power. Complete ionisation of particles above 150 nm is not reached with any plasma power. Figure 6 shows the normalised integrated ICP-MS signal intensities versus the normalised volume at three different plasma forward powers for stepwise removal of the large particle fractions from the aerosol. The effect of plasma forward power optimisation can be expressed by linear regression of the normalised signal intensities versus volume, where a higher slope indicates better vaporisation and ionisation of particles. Figure 6 shows that the energy transfer at 1000 W is less suitable to vaporise and ionise particles than 1300 W, and 1600 W is somewhere in between the two other settings. However, it should be noticed that uncertainties of the measurements overlap between all three power settings.

Single hole ablation experiments using different plasma forward powers all show the same characteristics with correlation of the integrated ICP-MS signal intensities and total particle volume after 100 to 120 laser pulses, indicating complete ionisation of particles smaller than 90 nm for all three plasma forward powers. Figure 7 shows variations in vaporisation indices (α) for different plasma forward power settings. Especially for 1600 W, overlapping error bars make it difficult to compare the results for different power settings. However, a trend to high vaporisation indices at 1000 W indicates most incomplete vaporisation and ionisation at this power setting (see Th, Hf, Zr, Al).

In general it can be concluded that the ICP vaporises the more volatile elements from all particle size fractions more efficiently. However, the data give no evidence that this selective extraction is completely taking place within the ICP, and chemical separation due to the ablation process must also be considered as a source of volatilisation. In any case the studies show that a significant portion of the aerosol entering the plasma is not completely ionised in the ICP. The available flexibility in ICP-MS operating conditions does not allow one to overcome the problem.

Conclusions

Glass particles smaller than about 90 nm can be vaporised and ionised completely in an inductively coupled plasma. This size limit was determined to be at 90 nm due to the fact that after the first 100 ablation pulses all aerosol particles are smaller than 90 nm for a NIST 610 sample and integrated ICP-MS signal intensities and the corresponding particle volumes are proportional. Experiments using a particle separation device show incomplete vaporisation and ionisation of large aerosol particles down to 150 nm. This limit is given by the separation device, which cannot remove particles smaller than 150 nm at the carrier gas flows applicable for ICP-MS.

Plasma forward power settings from 1000 W to 1600 W indicate that the most efficient particle vaporisation and ionisation occurs at 1300 W. The introduction of the vaporisation index (α), which indicates the deviation between complete and incomplete vaporisation and ionisation, shows inverse correlation to the elemental fractionation index. The correlation for a representative number of elements over the entire mass range indicates that elements with the lowest fractionation index relative to Ca (Fryer et al. [24]) show significant "incomplete" ionisation ($\alpha \approx 15$), whereas Pb as one of the most fractionating elements gives $\alpha \approx 0$. These results allow use to conclude that stoichiometric sampling by the laser into transportable particle size fractions below 150 nm (for silicates) are requirements to further reduce elemental fractionation as well as matrix independency.

Acknowledgements This work was supported by ETH Zürich and the Swiss National Science Foundation.

References

1. Becker JS (2002) J Anal At Spectrom 17:1172–1185
2. Jeffries TE, Perkins WT, Pearce NJG (1995) Analyst 120:1365–1371
3. Günther D, Frischknecht R, Heinrich CA, Kahlert HJ (1997) J Anal At Spectrom 12:939–944
4. Russo RE, Mao XL, Gonzalez JJ, Mao SS (2002) J Anal At Spectrom 17:1072–1075
5. Eggins SM, Kinsley LPJ, Shelley JMG (1998) Appl Surf Sci 129:278–286
6. Bleiner D, Günther D (2001) J Anal At Spectrom 16:449–456
7. Günther D (2002) Anal Bioanal Chem 372:31–32
8. Rodushkin I, Axelsson MD, Malinovsky D, Baxter DC (2002) J Anal At Spectrom 17:1223–1230
9. Rodushkin I, Axelsson MD, Malinovsky D, Baxter DC (2002) J Anal At Spectrom 17:1231–1239
10. Stirling CH, Lee DC, Christensen JN, Halliday AN (2000) Geochim Cosmochim Acta 64:3737–3750
11. Figg D, Kahr MS (1997) Appl Spectrosc 51:1185–1192
12. Guillong M, Günther D (2002) J Anal At Spectrom 17:831–837
13. Kuhn H-R, Günther D (2003) Anal Chem 75:747–753
14. Cromwell EF, Arrowsmith P (1995) Anal Chem 67(1):131–138
15. Jeong SH, Borisov OV, Yoo JH, Mao XL, Russo AE (1999) Anal Chem 71:5123–5130
16. Olesik JW, Dziewatkoski MP, Mcgowan GJ (1994) Abstr Pap Am Chem Soc 208:147-ANYL
17. Knight K, Chenery S, Zochowski SW, Thompson M, Flint CD (1996) J Anal Atom Spectrom 11(1):53–56
18. Horn I, Guillong M, Günther D (2001) Appl Surf Sci 182: 91–102
19. Guillong M, Horn I, Günther D (2003) J Anal At Spectrom 18(10):1224–1230
20. Jackson SE, Günther D (2003) J Anal At Spetrom 18:205–212
21. Aeschliman DB, Houk RS (2003) J Anal At Spectrom (Advance Article)
22. Guillong M, Kuhn H-R, Günther D (2002) Spectrochim Acta Part B Atom Spectrosc 58:211–220
23. Horn I, Günther D (2003) Appl Surf Sci 207:144–157
24. Fryer BJ, Jackson SE, Longerich HP (1995) Can Mineral 33: 303–312